Supplementary Materials for

Inhibition of PRC2 Activity by a Gain-of-Function H3 Mutation Found in Pediatric Glioblastoma

Peter W. Lewis, Manuel M. Müller, Matthew S. Koletsky, Francisco Cordero, Shu Lin, Laura A. Banaszynski, Benjamin A. Garcia, Tom W. Muir, Oren J. Becher, C. David Allis*

*To whom correspondence should be addressed. E-mail: alliscd@rockefeller.edu

Published 28 March 2013 on *Science* Express
DOI: 10.1126/science.1232245

This PDF file includes

SUPPLEMENTAL INFORMATION

MATERIALS/METHODS

Transgenic cell line generation

Human 293T, 293 or murine PDGF-transduced glioblastoma cells were transduced with recombinant, concentrated Lentivirus made with the pCDH-EF1-MCS-Puro or Neo expression vector (5μg / mL polybrene, 2x10^7 IFU). Transduced cells were grown under selection (1μg/mL Puromycin or 0.8μg/mL G418) at 24 hours post transduction for 72 hours. Cells were collected at 7-10 days post transduction for immunoblot analysis. The amino acid sequence of epitope tagged-H3.3 used in transgenic experiments (C-terminal FLAG and HA epitope sequences are bold and underlined):

M A R T K Q T A R K S T G G K A P R K Q L A T K A A R K S A P S T
G G V K K P H R Y R P G T V A L R E I R R Y Q K S T E L L I R K L
P F Q R L V R E I A Q D F K T D L R F Q S A A I G A L Q E A S E A
Y L V G L F E D T N L C A I H A K R V T I M P K D I Q L A R R I R G
E R A A A A G G **D Y K D D D D K S** A A G G **Y P Y D V P D Y A**

RCAS modeling of murine glioblastomas

To generate murine brainstem gliomas with and without the H3.3K27M mutation, we injected 1 µL ($1x10^5$ cells) of RCAS-PDGF-B, RCAS-Cre, ± RCAS-H3.3K27M expressing DF1 cells intracranially into nestin tv-a; p53 floxed neonatal mice. Mice were monitored carefully for signs of tumor development (hydrocephalus, lethargy, head tilt). On the appearance of brain tumor symptoms (or at 12 weeks if mice did not develop symptoms), mice were euthanized with CO_2, brain tissue was extracted, fixed in formalin, and paraffin embedded or alternatively tumor tissue was dissected, and snap-frozen for western analysis. All animal experiments were in accordance with approved animal protocol by Duke's IACUC (A239-10-9).

Immunohistochemistry

Immunohistochemistry on mouse and human formalin-fixed, paraffin-embedded sections was performed using Discovery XT (Ventana Medical Systems). H3K27me3 antibody (cell signaling) dilution was 1:200. Quantification of staining was done with Metamorph.

Human DIPG tissue was obtained from Memorial Sloan-Kettering Cancer Center, New York University Medical Center (Drs. Karajannis and Zagzag), Children's Memorial hospital (Dr. Fangusaro), University of Colorado (Dr. Foreman) and was IRB approved at the respective institutions.

Peptide crosslinking

1μg of purified PRC2 was incubated with 2μg of photoMet or benzophenone biotinylated peptide in crosslinking buffer (Final volume 30μL) in opaque 1.5mL microfuge tubes. A 6W handheld UV crosslinking was placed directly onto tubes and used to irradiate the sample with long wavelength UV light for 5 or 10 minutes on ice. Samples were resolved by SDS-PAGE and transferred to nitrocellulose followed by Streptavidin-HRP incubation.

Peptide pulldown assays

40μL of high capacity Streptavidin-Sepharose beads containing saturating amounts of biotinylated H3 18-27 peptides (unmodified, K27M, K27ac, K27me3) were added to 1mL of clarified concentrated HeLa nuclear extract (8.7mg/mL). Following a 4-hour incubation at 4C, the beads were collected and washed three times in 1mL of buffer (20mM HEPES 7.9, 50mM KCl, 1mM EDTA, 0.01% NP-40, 2mM 2-mercaptoethanol, 0.4mM PMSF). Bound protein was eluted with 1x SDS loading buffer. Highly purified GST-EED (WD domain) or GST-CBX7 (chromodomain) (10μg) was added to the 40μL of peptide bound Streptavidin-Sepharose beads. Incubation, wash and elution conditions were followed as described.

Biacore measurements

Saturating amounts of 3 peptides (18-37 unmodified, K27me3, or K27M) were immobilized on SA Biacore chip (GE Healthcare). Purified recombinant GST fusion protein containing the WD-domain of human EED dialyzed in 1xPBS was used for all measurements. Interaction measurements were taken in triplicate with GST-EED concentrations of 0.2μM, 2μM, 10μM, 20μM and 200μM in 1xPBS. Kinetic and affinity constants were determined using BIAevaluation software.

Peptide Synthesis

Peptides were synthesized on a Rink amide-MBHA resin using 2-(1H-benzotriazole-1-yl)-1,1,3,3-tetramethyluronium hexafluorophosphate (HBTU) activation of N^{α}-Fmoc protected amino acids. For photo-crosslinker peptides, a C-terminal N^{α}-Fmoc-Lys(N^{ε}-alloc) residue allowed for biotin incorporation upon selective alloc removal from a 4-mer peptide intermediate by treatment with Pd(0). Fmoc-photo-L-Methionine (synthesized from L-photo-Methionine (Pierce) as published previously (Vila-Perelló et al. JACS, **129** 8068)) and Fmoc-4-benzoyl-L-phenylalanine (AdvancedChemTech) were coupled with 2-(1H-7-Azabenzotriazole-1-yl)-1,1,3,3-tetramethyluronium hexafluorophosphate (HATU) for the synthesis of peptides **1** and **2**, respectively. Peptide N-termini were acetylated using acetic anhydride. The resulting peptides were cleaved with TFA containing 5% triisoproylsilane (TIS) for one hour at RT, precipitated with ether and purified by preparative reverse-phase HPLC (RP-HPLC) on a C-18 column with a 5-35% B gradient (Solvent B: 90% acetonitrile, 10% H_2O, 0.1% trifluoroacetic acid; Solvent A: H_2O containing 0.1% trifluoroacetic acid). Purity of the final product was assessed by C-18 RP-HPLC using a 0-30% B (benzophenone-containing peptide **2**) or 0-40% (photo-Met containing peptide **1**) gradient. Peptide identity was confirmed by electrospray ionization mass spectrometry (ESI-MS; **1** calculated: 1536.80 Da, observed: 1536.83 Da; **2** calculated $M+H^+$: 1692.83 Da, observed: 1692.85 Da).

Selective biotinylation of the K27nle peptide **3** at its C-terminal lysine residue was achieved upon orthogonal MTT removal by 1% TFA in CH_2Cl_2 in the full-length, N-terminally acetylated peptide before cleavage. Peptide **3** was cleaved from the resin by incubation with 95% TFA containing 2.5% TIS and 2.5% H_2O for 1.5 hours at RT. Purification by preparative reverse-phase HPLC (RP-HPLC) on a C-18 column with a X-XX% B gradient yielded pure peptide (calculated $M+H^+$: 2571.5 Da, observed: 2571.5 Da).

SUPPLEMENTAL FIGURE LEGENDS

Fig. S1 Generation of H3K27M-specific antisera. **(A)** Shown are immunoblots of whole cell extract from the indicated transgenic 293T cell lines. The H3K27M-specific antisera was generated in collaboration with EMD Millipore (Temecula, CA). The H3K27M rabbit antiserum was used at a concentration of 1:1000. **(B)** Immunoblot of acid extracted histones from four different human DIPG samples with the anti-K27M antibody. Fraction of H3.3K27M to the total amount of histone H3 in human DIPG samples as measured by quantitative mass spectrometry. **(C)** Proliferating ectopic cell clusters but no tumor formation with K27M H3.3 expression + p53 loss in the postnatal murine brainstem. Representative high magnification (40X) double immunofluorescence for HA (H3.3 K27M) and PCNA demonstrating an ectopic cell cluster containing K27M-positive cells and PCNA-positive cells. **(D)** Representative high magnification (40X) double immunofluorescence for HA (H3.3 WT) and PCNA demonstrating the absence of PCNA-positive cells around H3.3-WT-positive cells.

Fig. S2 PRC2 components remain unchanged in H3.3K27M transgenic PDGF-driven murine glioblastoma cell line (**A**). Shown are immunoblots with antisera specific to PRC2-associated proteins AEBP2 and Jarid2, and core PRC2 subunits, EED, EZH2 and SUZ12. **(B)** Chromatin containing endogenous, wildtype H3 exhibits reduced H3K27me3 or H3K9me3 levels. 293T cells were transduced with lentiviruses expressing H3.2-HA-FLAG and untagged H3.3 K9M, K9R, K27M, or K27R. Immunoprecipitated oligonucleosomes (anti-FLAG) were immunoblotted for H3K9me3, H3K27me3 or general H3. **(C)** H3.3 G34R/V mutations decrease H3K36me2/3 levels. Quantitative mass-spectrometry of H3K36me3 levels on immunoprecipitated transgenic H3.3 proteins from purified heterotypic mononucleosomes. **(D)** Purified human GST-SET2 (aa 1410-1714) from E.coli. **(E)** Reduced hSET2 activity on heterotypic G34R/V mononucleosomes. Recombinant human SET2 (200ng) or PRC2 (50ng) were used for methyltransferase assays on wildtype H3.3 or heterotypic G34R or G34V mononucleosomes.

Fig. S3 Purified components for *in vitro* PRC2 histone methyltransferase assays. **(A)** Silver stain of peak PRC2 and EED-Y365A complex Mono Q fraction. PRC2 was purified using both affinity and conventional chromatography from a HeLa cell line that expresses epitope-tagged EED. **(B)** Coomassie stained gel of purified mono- or oligonucleosomes from epitope-tagged 293T cells. **(C)** Heterotypic H3.3K27M heterotypic mononucleosomes or H3.3K27M-containing oligonucleosomes are poor substrates for PRC2 methyltransferase activity. Fluorography of PRC2-mediated methylation of wildtype H3.3 or H3.3K27M nucleosome substrates. **(D,E)** Titration of increasing concentration of K27M or K27ac peptide, while simultaneously decreasing the concentration of K27me3 peptide. We observed a modest decrease in PRC2 activity at a K27M:K27me3 ratio of 1:2.3 that steadily grew with an increased ratio of K27M to K27me3 peptide. In contrast, no decrease in PRC2 activity was observed at a 9:1 ratio of K27ac: K27me3 peptide.

Fig. S4 Probing interaction between K27M and PRC2 components. **(A)** No observable interaction between PRC2 and K27M in peptide pulldown assay from HeLa cell nuclear extract. EZH2 and SUZ12 immunoblot of eluate from peptide pulldowns using the indicated peptides. **(B)** No observable interaction between GST-EED and K27M in peptide pulldown assay. Coomassie stained gel of eluate from pulldowns between GST-EED and the indicated peptides. **(C)** No observable interaction between PRC1 component CBX7 and K27M in peptide pulldown. Coomassie gel of eluate from pulldowns between GST-CBX7 and the indicated peptides. **(D)** No observable interaction between EED and K27M peptide by Biacore (SPR). The H3K27me3 peptide interacted with EED with a measured Kd = 38 +/- 7.4 μM. **(E)** Benzophenone H3K27M peptide crosslinks EZH2. Coomassie gel of PRC2 complex (left), and streptavidin-HRP blot (right). **(F)** Structure of PhotoMet peptide **1** used in figure 4A. **(G)** Structure of benzophenone K27M peptide (**2**) used in Fig. 4SE.

Fig. S5 PRC2 containing Y365A EED mutant is sensitive to K27M inhibition. **(A)** Purified PRC2 complexes (wildtype EED or Y365A EED) were incubated with either wildtype or K27M heterotypic mononucleosomes or oligonucleosomes. Shown are fluorography and coomassie gels of the reactions. **(B)** Interactions between the base of Histone H3 (31-42)

and SUZ12 was recently reported to allosterically stimulate PRC2 activity. K27M inhibits allosteric activation by H3.3 (31-42) peptide. Purified wildtype PRC2 was incubated with wildtype mononucleosomes and the indicated peptides at 90μM. The H3K27M peptide was added at a concentration of 45μM. Shown are fluorography and coomassie gels of the reactions.

Fig. S6 **(A)** Peptide structure of the H3K27Nle peptide **3** used in figure 4B. **(B)** Immunoblot for H3K27me3 of whole 293T cells transduced with H3.3, H3.3K27M, H3.3K27I or H3.3K27L. Anti-HA shows the relative amounts of the H3.3 transgenes. **(C)** Fluorography of methyltransferase reactions with PRC2 and wildtype H3.3 mononucleosomes in the presence of 20μM or 50μM H3 (18-37) peptide containing K27acetyl, K27Met, K27Nle, K27Ile or K27Leu. **(D)** Fluorography of PRC2 methyltransferase reactions with reconstituted nucleosomes containing recombinant human histones H3, H2B, H2A and H4. Reactions also contain 100μM H3 peptides (18-37) containing K27acetyl, K27Ile, K27Met, K27Nle, or K27Leu. **(E)** Structural homology modeling of the human EZH2 active site using the web-based Phyre (BBSRC) program. The human SET8-H4K20 co-crystal structure was used for modeling (*14*). Active aromatic residues F724, Y726, Y641 and F667 are shown. A methionine was modeled in place of the H4K20 from the original SET8 co-crystal structure. Stick diagrams for L-leucine, L-isoleucine, L-methionine and L-norleucine are shown. (**F**) Coomassie gel of purified wildtype or Y641N-containing PRC2 from Hela cells transduced with FLAG-EZH2 or FLAG-EZH2-Y641N.

Fig. S7 Inhibition of K9me2, K27me2 and K36me2 by K9M, K27M and K36M transgenes, respectively. **(A)** Shown are immunoblots of whole cell extract from lentiviral transduced 293T cells expressing the indicated H3.3 transgenes. **(B)** The K3K9M peptide does not inhibit PRC2-dependent nucleosome methylation. K9M or K27M peptides were added to PRC2 reactions with wildtype mononucleosomes at 10μM or 45μM. **(C)** Coomassie gels of GST-hSUV39H1 (aa 82-412) and GST-hG9a (aa 530-1210). IC_{50} measurement for SUV39H1 and G9a with the H3K9M (1-20) peptide (IC_{50} for K9M = 2.2μM for SUV39H1 (95% CI: 1.7-2.6); IC_{50} for K9M = 3.6μM (95% CI: 2.1-5.9) for G9a).

Fig. S8 Chromatin context of the K-to-M H3 sequence is important for in vivo inhibition of trimethylation. The H3 tail (aa 1-42) was cloned onto the core domain (aa 23-102) of histone H4-HA-FLAG. The H3-H4 hybrid genes containing the K-to-M or K-to-R mutations were expressed in 293T cells. **(A)** Immunoblots of whole cell extract of H3.3 K9M, K9R and the K9M, K9R H3-H4 hybrid 293T cells. **(B)** Immunoblots of whole cell extract of H3.3 K27M, K27R and the K27M, K27R H3-H4 hybrid 293T cells. **(C)** Immunoblots of whole cell extract of H3.3 K36M, K36R and the K36M, K36R H3-H4 hybrid 293T cells. **(D)** H3K9me3 levels were reduced in cells expressing the K9M H3-H4 hybrid. However, little reduction in H3K27me3 or H3K36me3 levels was observed with the hybrid H3-H4 transgenes **(B,C)**. To determine if the position of the K-to-M mutation on the N-terminal tail of the hybrid H3-H4 protein, we constructed a second set of hybrid transgenes. The first 14 residues of the H3 tail were replaced by 14 amino acids surrounding the K27 or K36 (H3-H4-K36 (K9) or H3-H4-K27 (K9)) **(D)**. The K-to-M mutations in these hybrids also failed to reduce K27me3 or K36me3 levels **(B,C)**. These results suggest that the position of the K-to-M H3 tail on the nucleosome is critical for full inhibition activity.

Figure S1

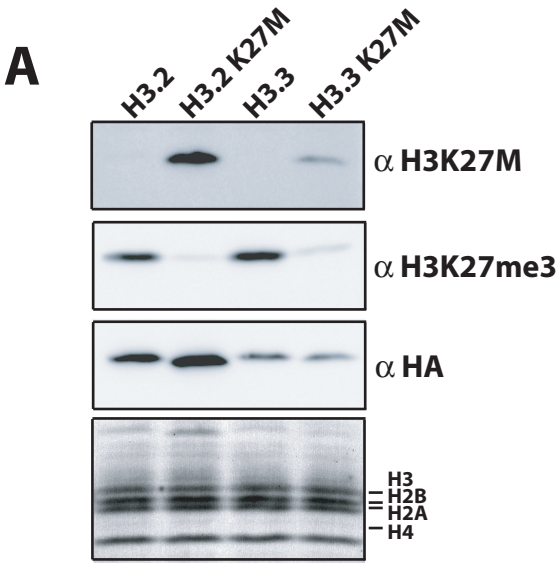

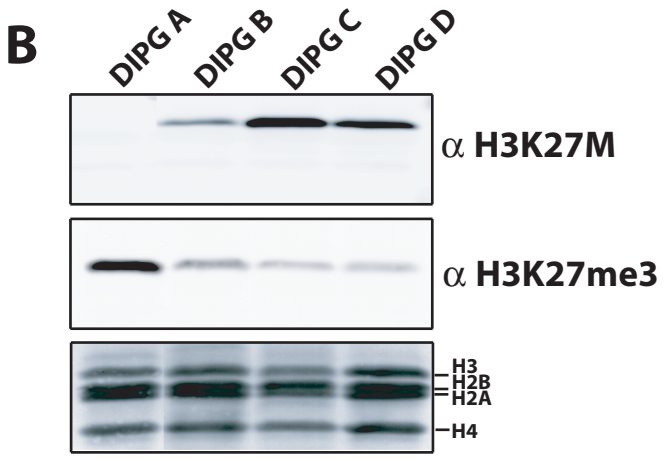

		Mutant % out of total H3	
Sample	**Genotype**	**Average**	**STDEV**
DIPG A	wt	-	-
DIPG B	K27M H3.1	3.63%	0.33%
DIPG C	K27M H3.3	17.61%	1.11%
DIPG D	K27M H3.3	6.24%	1.24%

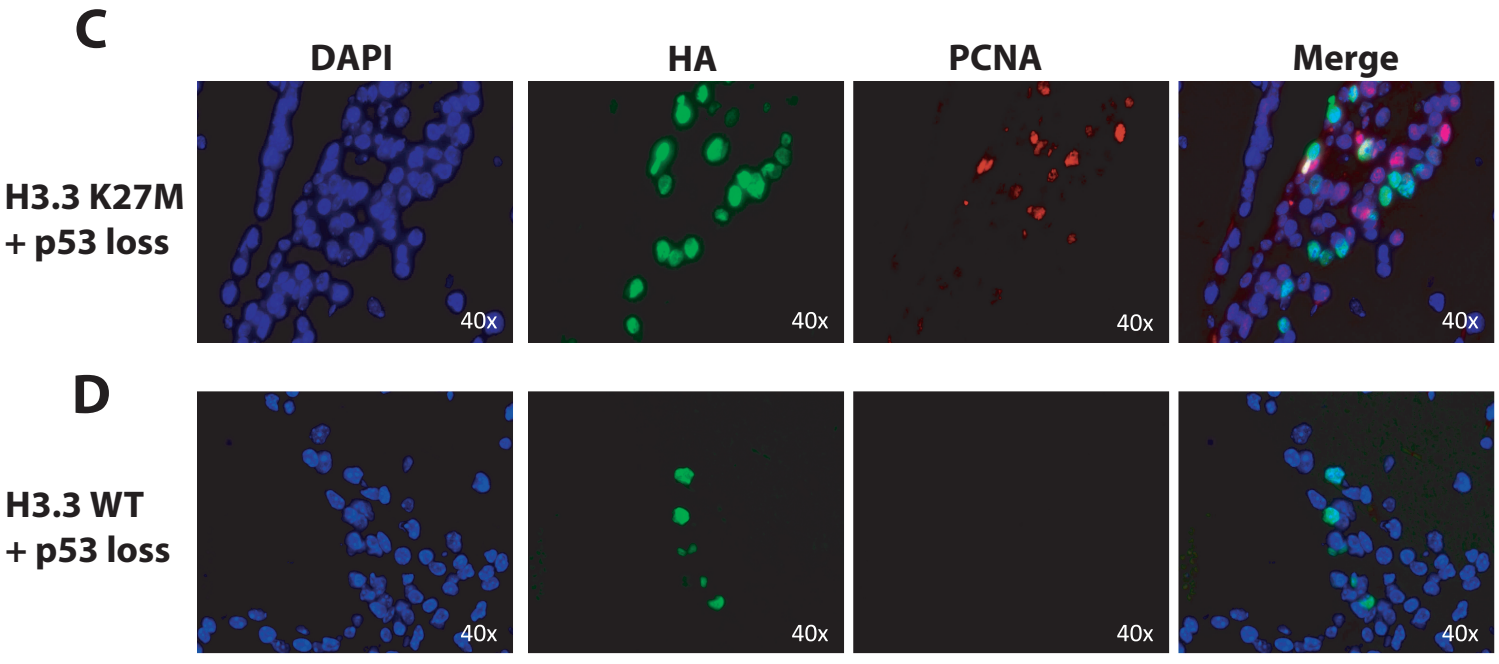

Figure S2

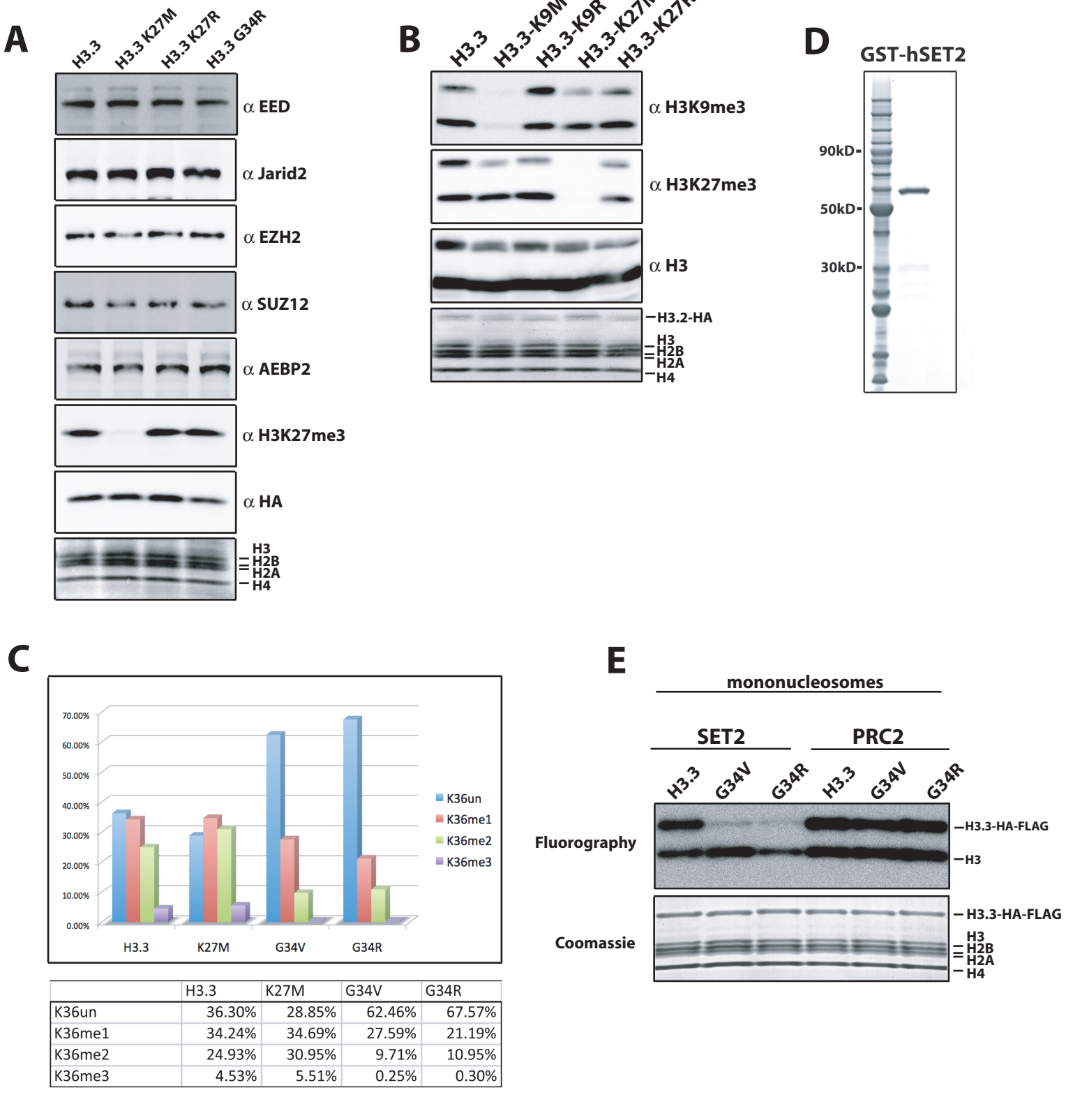

	H3.3	K27M	G34V	G34R
K36un	36.30%	28.85%	62.46%	67.57%
K36me1	34.24%	34.69%	27.59%	21.19%
K36me2	24.93%	30.95%	9.71%	10.95%
K36me3	4.53%	5.51%	0.25%	0.30%

Figure S3

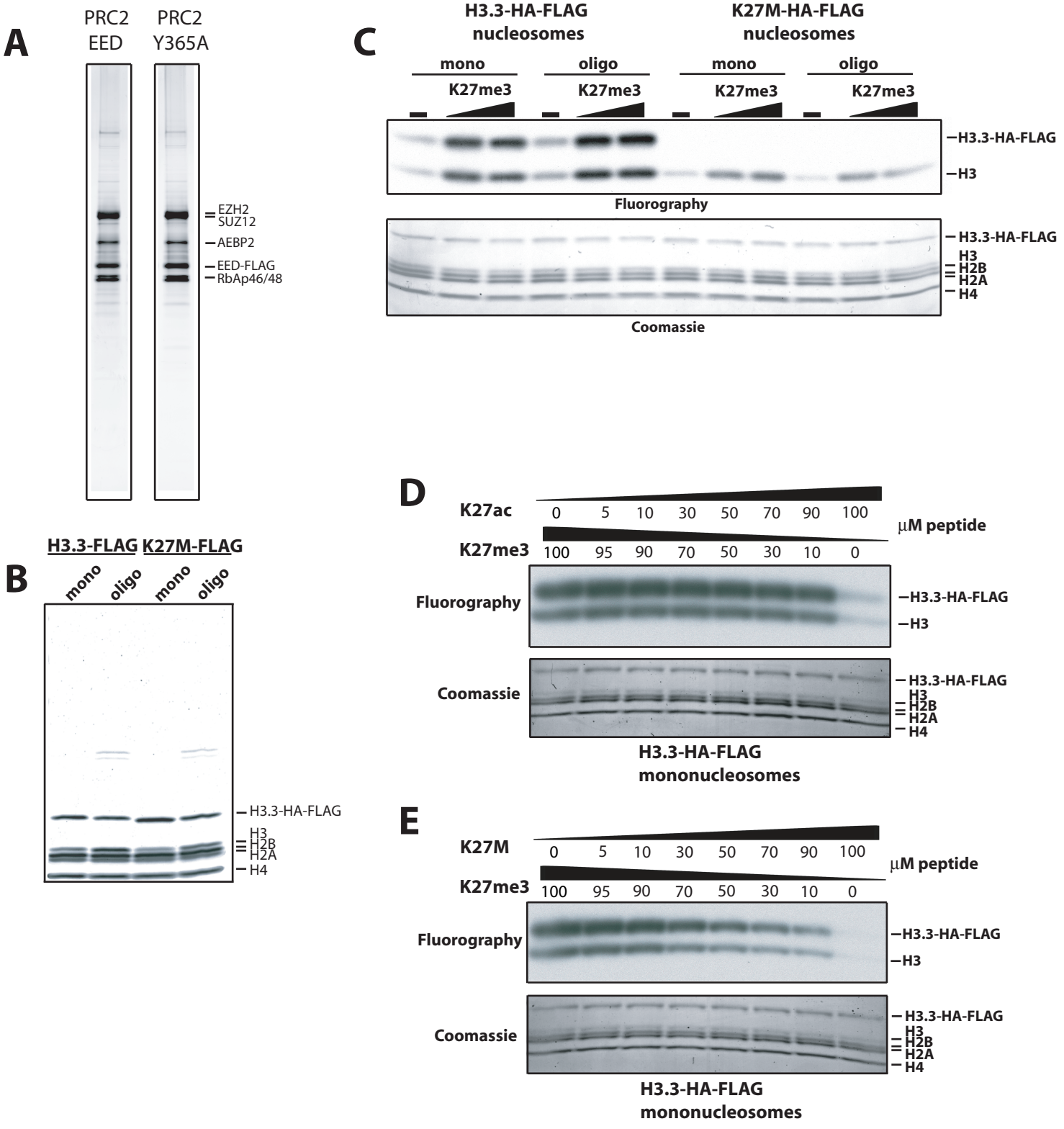
A
PRC2 EED
PRC2 Y365A
EZH2
SUZ12
AEBP2
EED-FLAG
RbAp46/48
B
H3.3-FLAG K27M-FLAG
mono
oligo
mono
oligo
H3.3-HA-FLAG
H3
H2B
H2A
H4
C
H3.3-HA-FLAG nucleosomes
K27M-HA-FLAG nucleosomes
mono
oligo
mono
oligo
K27me3
K27me3
K27me3
K27me3
H3.3-HA-FLAG
H3
Fluorography
H3.3-HA-FLAG
H3
H2B
H2A
H4
Coomassie
D
K27ac
0 5 10 30 50 70 90 100
μM peptide
K27me3
100 95 90 70 50 30 10 0
Fluorography
H3.3-HA-FLAG
H3
Coomassie
H3.3-HA-FLAG
H3
H2B
H2A
H4
H3.3-HA-FLAG mononucleosomes
E
K27M
0 5 10 30 50 70 90 100
μM peptide
K27me3
100 95 90 70 50 30 10 0
Fluorography
H3.3-HA-FLAG
H3
Coomassie
H3.3-HA-FLAG
H3
H2B
H2A
H4
H3.3-HA-FLAG mononucleosomes

Figure S4

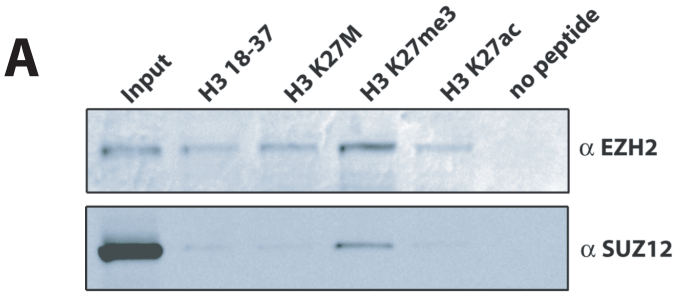

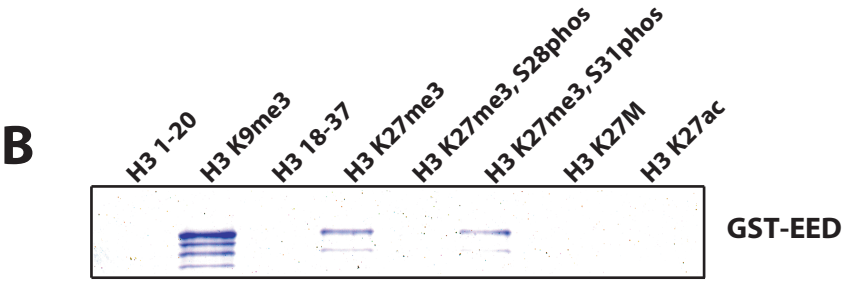

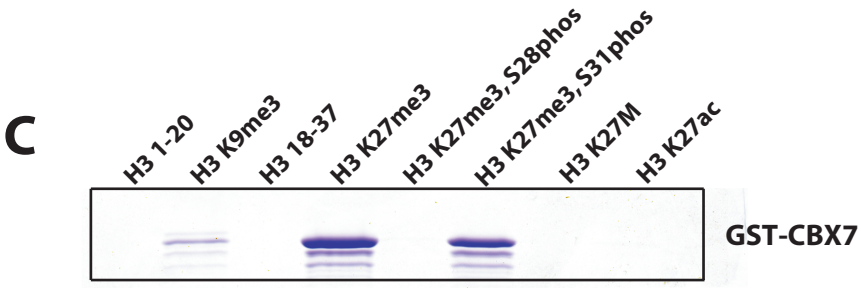

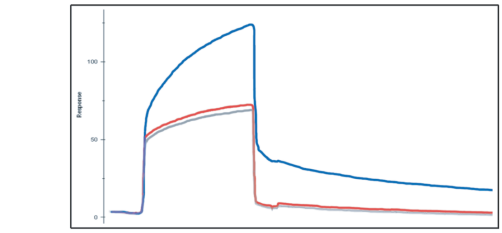

Peptide	Binding μM
H3 (18-37)	>300
K27me3	38 +/- 7.4
K27M	>300

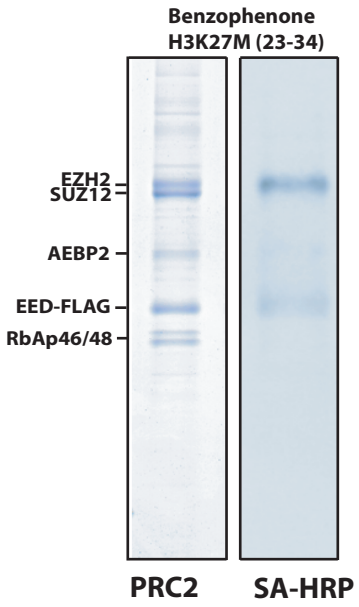

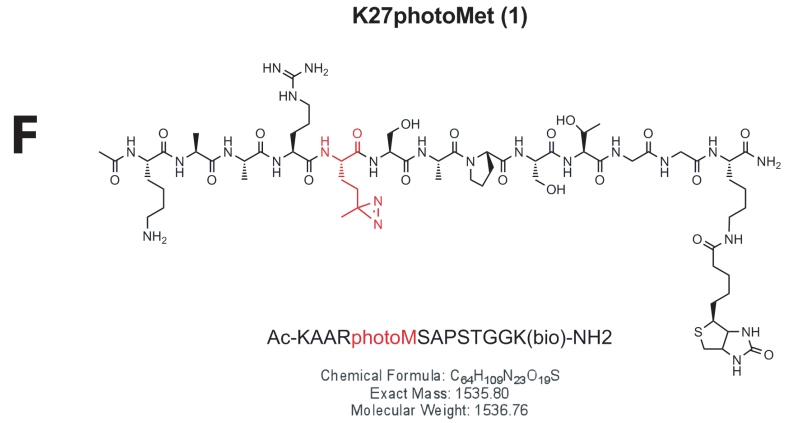

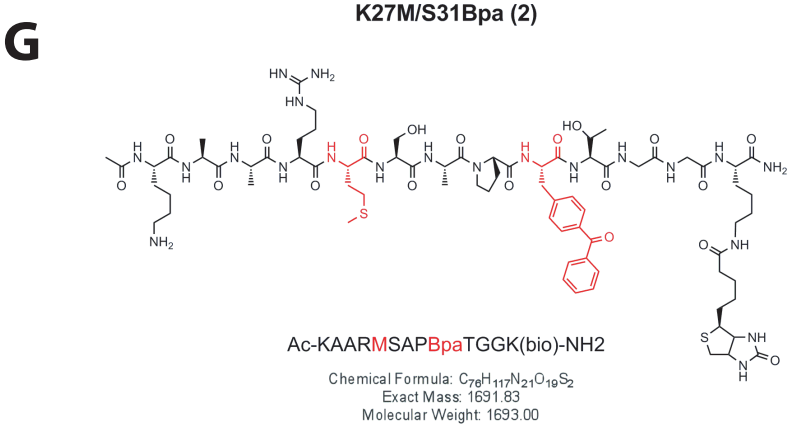

Figure S5

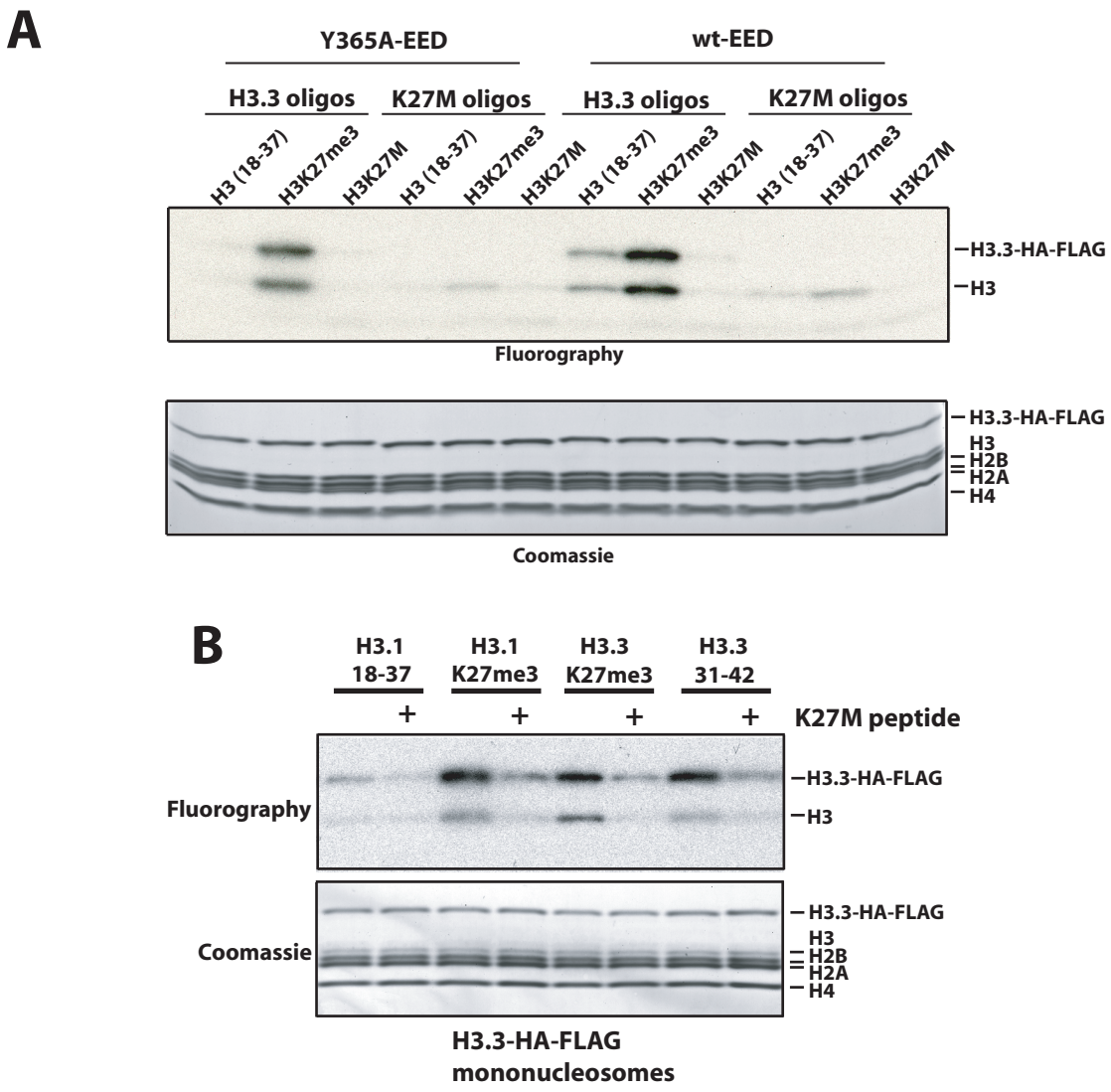
A
Y365A-EED
wt-EED
H3.3 oligos
K27M oligos
H3.3 oligos
K27M oligos
H3 (18-37)
H3K27me3
H3K27M
H3 (18-37)
H3K27me3
H3K27M
H3 (18-37)
H3K27me3
H3K27M
H3 (18-37)
H3K27me3
H3K27M
H3.3-HA-FLAG
H3
Fluorography
H3.3-HA-FLAG
H3
H2B
H2A
H4
Coomassie
B
H3.1 18-37
H3.1 K27me3
H3.3 K27me3
H3.3 31-42
+
+
+
+
K27M peptide
Fluorography
H3.3-HA-FLAG
H3
Coomassie
H3.3-HA-FLAG
H3
H2B
H2A
H4
H3.3-HA-FLAG mononucleosomes

Figure S6

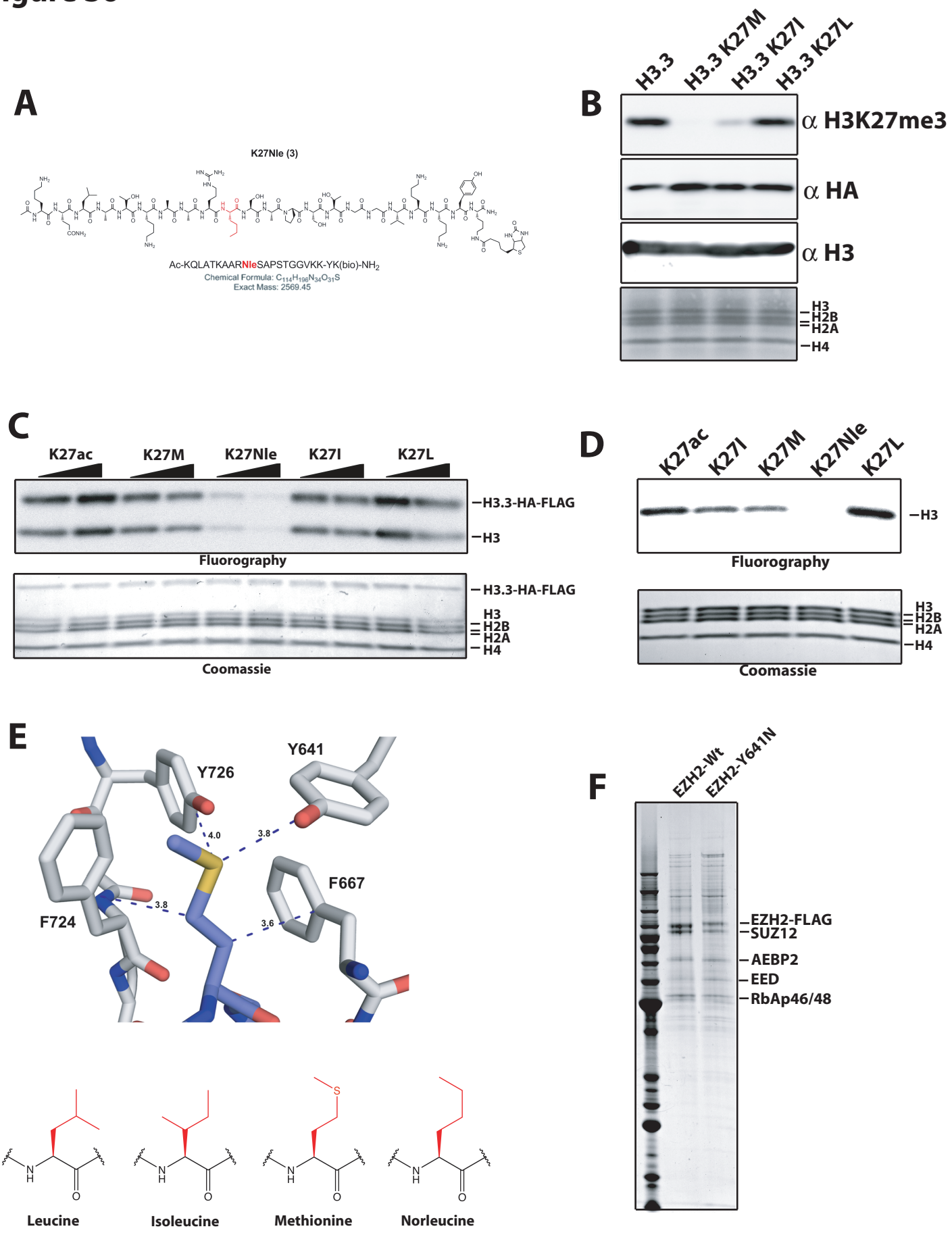
A
K27Nle (3)
Ac-KQLATKAARNleSAPSTGGVKK-YK(bio)-NH2
Chemical Formula: C114H196N34O31S
Exact Mass: 2569.45
B
H3.3
H3.3 K27M
H3.3 K27I
H3.3 K27L
α H3K27me3
α HA
α H3
H3
H2B
H2A
H4
C
K27ac
K27M
K27Nle
K27I
K27L
H3.3-HA-FLAG
H3
Fluorography
H3.3-HA-FLAG
H3
H2B
H2A
H4
Coomassie
D
K27ac
K27I
K27M
K27Nle
K27L
H3
Fluorography
H3
H2B
H2A
H4
Coomassie
E
Y726
Y641
F667
F724
4.0
3.8
3.8
3.6
Leucine
Isoleucine
Methionine
Norleucine
F
EZH2-Wt
EZH2-Y641N
EZH2-FLAG
SUZ12
AEBP2
EED
RbAp46/48

Figure S7

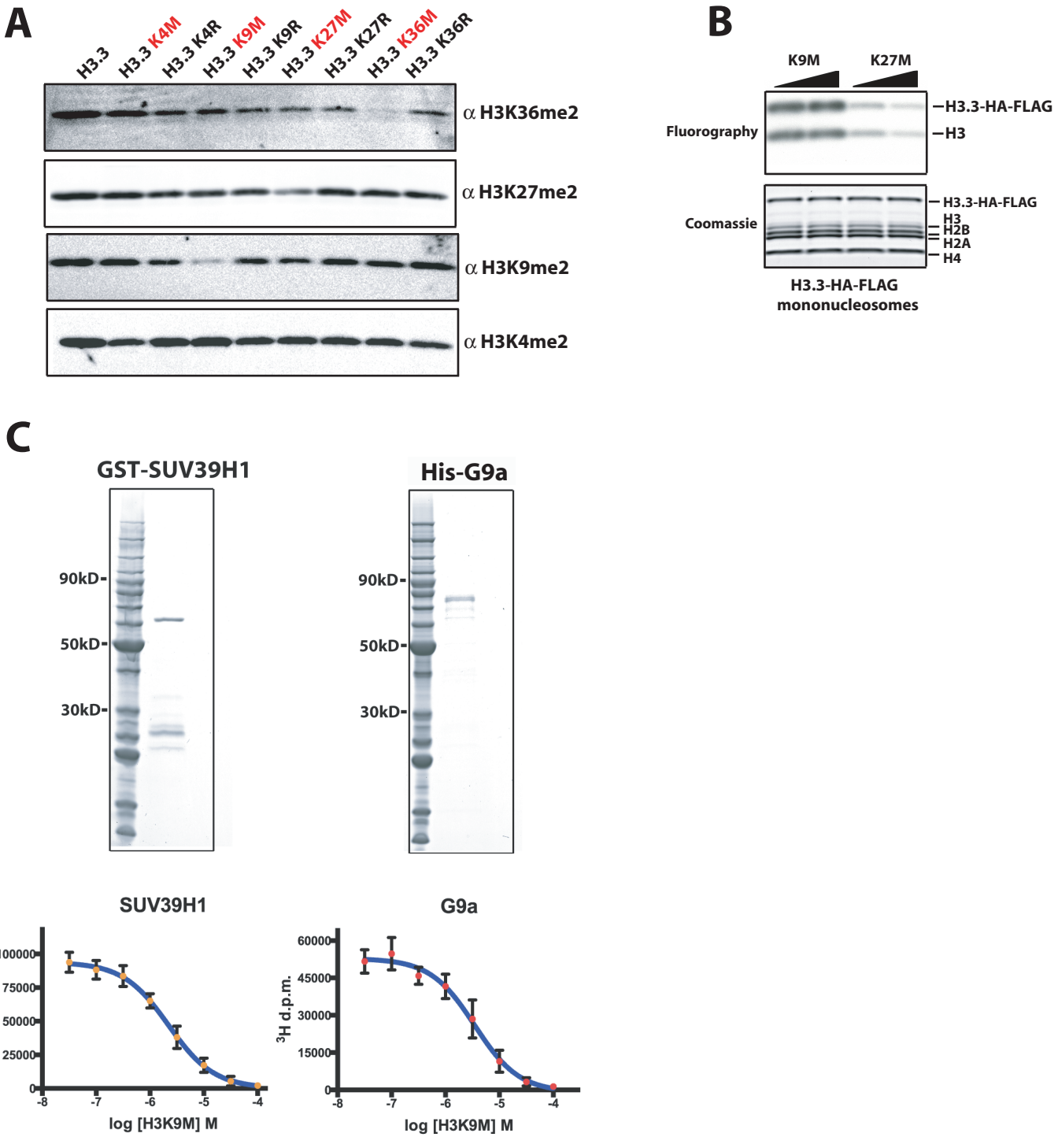
A
H3.3
H3.3 K4M
H3.3 K4R
H3.3 K9M
H3.3 K9R
H3.3 K27M
H3.3 K27R
H3.3 K36M
H3.3 K36R
α H3K36me2
α H3K27me2
α H3K9me2
α H3K4me2
B
K9M
K27M
Fluorography
H3.3-HA-FLAG
H3
Coomassie
H3.3-HA-FLAG
H3
H2B
H2A
H4
H3.3-HA-FLAG
mononucleosomes
C
GST-SUV39H1
His-G9a
90kD
50kD
30kD
SUV39H1
G9a
3H d.p.m.
log [H3K9M] M

Figure S8

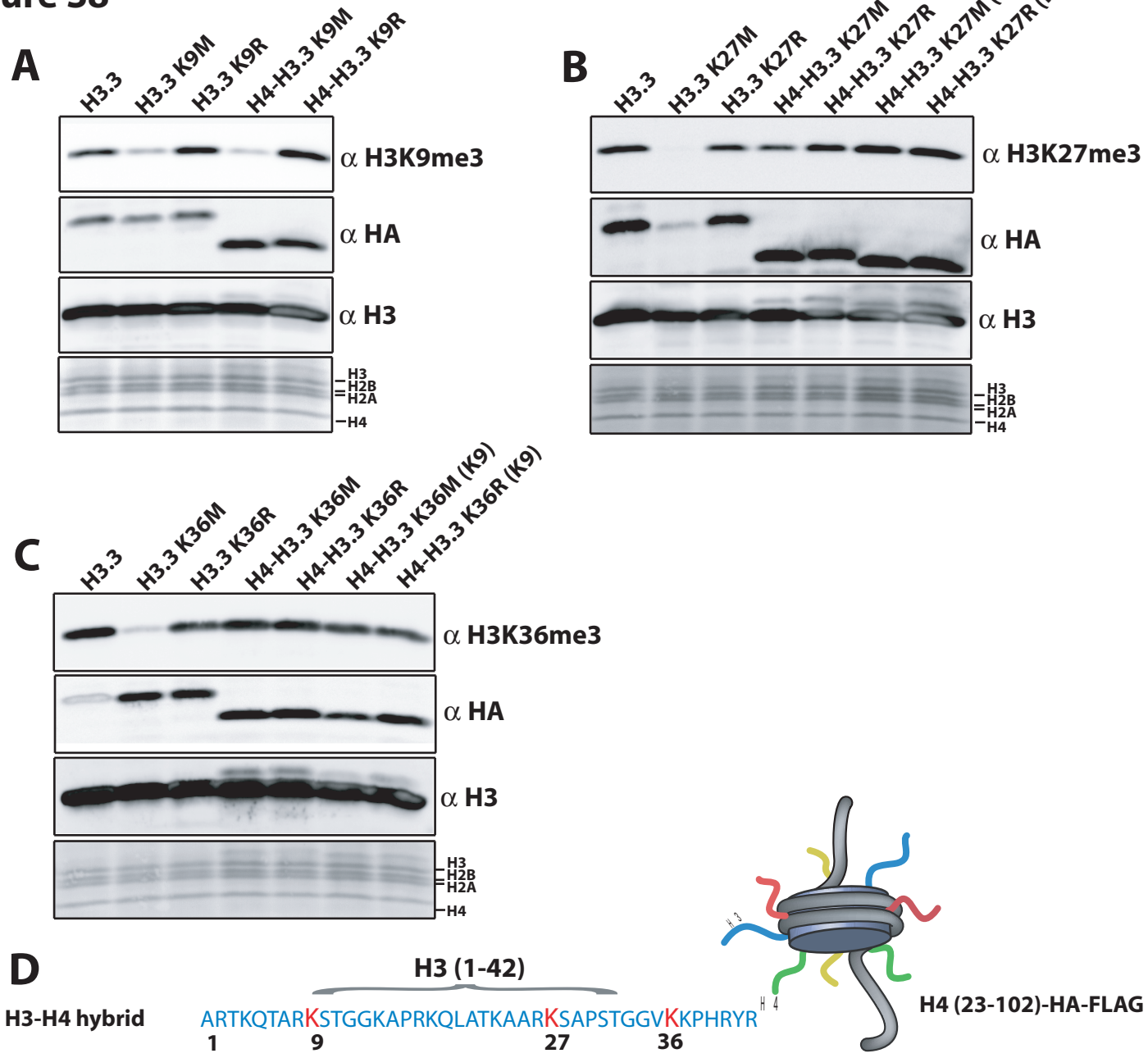

H4 (23-102)-HA-FLAG

D

H3 (1-42)

H3-H4 hybrid ARTKQTARKSTGGKAPRKQLATKAARKSAPSTGGVKKPHRYR

1 9 27 36

		Trimethylation Inhibition
H3-H4-K9R	ARTKQTARRSTGGKAPRKQLATKAARKSAPSTGGVKKPHRYR	–
H3-H4-K9M	ARTKQTARMSTGGKAPRKQLATKAARKSAPSTGGVKKPHRYR	+++
H3-H4-K27R	ARTKQTARKSTGGKAPRKQLATKAARRSAPSTGGVKKPHRYR	–
H3-H4-K27M	ARTKQTARKSTGGKAPRKQLATKAARMSAPSTGGVKKPHRYR	+
H3-H4-K36R	ARTKQTARKSTGGKAPRKQLATKAARKSAPSTGGVRKPHRYR	–
H3-H4-K36M	ARTKQTARKSTGGKAPRKQLATKAARKSAPSTGGVMKPHRYR	–
H3-H4-K36 (K9)	ARPSTGGVKKPHRYRPRKQLATKAARKSAPSTGGVKKPHRYR	–
H3-H4-K36R (K9)	ARPSTGGVRKPHRYRPRKQLATKAARKSAPSTGGVKKPHRYR	–
H3-H4-K36M (K9)	ARPSTGGVMKPHRYRPRKQLATKAARKSAPSTGGVKKPHRYR	–
H3-H4-K27 (K9)	ARATKAARKSAPSGGKPRKQLATKAARKSAPSTGGVKKPHRYR	–
H3-H4-K27R (K9)	ARATKAARRSAPSGGKPRKQLATKAARKSAPSTGGVKKPHRYR	–
H3-H4-K27M (K9)	ARATKAARMSAPSGGKPRKQLATKAARKSAPSTGGVKKPHRYR	–

References

1. S. J. Elsässer, C. D. Allis, P. W. Lewis, New epigenetic drivers of cancers. *Science* **331**, 1145 (2011). doi:10.1126/science.1203280 Medline

2. J. A. Simon, C. A. Lange, Roles of the EZH2 histone methyltransferase in cancer epigenetics. *Mutat. Res.* **647**, 21 (2008). doi:10.1016/j.mrfmmm.2008.07.010 Medline

3. R. Margueron, D. Reinberg, The Polycomb complex PRC2 and its mark in life. *Nature* **469**, 343 (2011). doi:10.1038/nature09784 Medline

4. D. A. Khuong-Quang *et al*., K27M mutation in histone H3.3 defines clinically and biologically distinct subgroups of pediatric diffuse intrinsic pontine gliomas. *Acta Neuropathol.* **124**, 439 (2012). doi:10.1007/s00401-012-0998-0 Medline

5. J. Schwartzentruber *et al*., Driver mutations in histone H3.3 and chromatin remodelling genes in paediatric glioblastoma. *Nature* **482**, 226 (2012). doi:10.1038/nature10833 Medline

6. G. Wu *et al*.; St. Jude Children's Research Hospital–Washington University Pediatric Cancer Genome Project, Somatic histone H3 alterations in pediatric diffuse intrinsic pontine gliomas and non-brainstem glioblastomas. *Nat. Genet.* **44**, 251 (2012). doi:10.1038/ng.1102 Medline

7. O. J. Becher *et al*., Preclinical evaluation of radiation and perifosine in a genetically and histologically accurate model of brainstem glioma. *Cancer Res.* **70**, 2548 (2010). doi:10.1158/0008-5472.CAN-09-2503 Medline

8. R. Margueron *et al*., Role of the polycomb protein EED in the propagation of repressive histone marks. *Nature* **461**, 762 (2009). doi:10.1038/nature08398 Medline

9. C. Xu *et al*., Binding of different histone marks differentially regulates the activity and specificity of polycomb repressive complex 2 (PRC2). *Proc. Natl. Acad. Sci. U.S.A.* **107**, 19266 (2010). doi:10.1073/pnas.1008937107 Medline

10. D. B. Yap *et al*., Somatic mutations at EZH2 Y641 act dominantly through a mechanism of selectively altered PRC2 catalytic activity, to increase H3K27 trimethylation. *Blood* **117**, 2451 (2011). doi:10.1182/blood-2010-11-321208 Medline

11. C. J. Sneeringer *et al*., Coordinated activities of wild-type plus mutant EZH2 drive tumor-associated hypertrimethylation of lysine 27 on histone H3 (H3K27) in human B-cell lymphomas. *Proc. Natl. Acad. Sci. U.S.A.* **107**, 20980 (2010). doi:10.1073/pnas.1012525107 Medline

12. S. D. Taverna, H. Li, A. J. Ruthenburg, C. D. Allis, D. J. Patel, How chromatin-binding modules interpret histone modifications: Lessons from professional pocket pickers. *Nat. Struct. Mol. Biol.* **14**, 1025 (2007). doi:10.1038/nsmb1338 Medline

13. A. Karytinos *et al*., A novel mammalian flavin-dependent histone demethylase. *J. Biol. Chem.* **284**, 17775 (2009). doi:10.1074/jbc.M109.003087 Medline

14. J. F. Couture, E. Collazo, J. S. Brunzelle, R. C. Trievel, Structural and functional analysis of SET8, a histone H4 Lys-20 methyltransferase. *Genes Dev.* **19**, 1455 (2005). doi:10.1101/gad.1318405 Medline